BNL-113518-2017-JA

CLOUD DROPLET ACTIVATION THROUGH OXIDATION OF ORGANIC AEROSOL INFLUENCED BY TEMPERATURE AND PARTICLE PHASE STATE

Slade, J. H., Shiraiwa, M., Arangio, A., Su, H., Pöschl, U., Wang, J., and Knopf, D. A.

Submitted for publication in
Geophy. Res. Lettrs

January 2017

Environmental & Climate Science Dept.

Brookhaven National Laboratory

U.S. Department of Energy
DOE Office of Science

DISCLAIMER

Cloud droplet activation through oxidation of organic aerosol influenced by temperature and particle phase state

Slade, Jonathan H.[1†], Shiraiwa, Manabu[2, 3], Arangio, Andrea[2], Su, Hang[2, 4], Pöschl, Ulrich[2], Wang, Jian[5], and Daniel A. Knopf[1*]

[1]Stony Brook University, Institute for Terrestrial and Planetary Atmospheres, School of Marine and Atmospheric Sciences, Stony Brook, NY

[2]Max Planck Institute for Chemistry, Multiphase Chemistry Department, Mainz, Germany

[3]University of California, Irvine, Department of Chemistry, Irvine, CA

[4]Institute for Environmental and Climate Research, Jinan University, Guangzhou, China

[5]Brookhaven National Laboratory, Department of Environmental and Climate Sciences, Upton, NY

[†]Now at Purdue University, Department of Chemistry, West Lafayette, IN

[*]To whom correspondence should be addressed.

Key Points

1. Hydrophobic-to-hydrophilic conversion of organic aerosol through oxidation is impacted by temperature and particle phase state.
2. Oxidation of organic aerosol below its glass transition increases particle hygroscopicity.
3. Cloud droplet number concentrations are influenced by temperature at which organic aerosol undergoes oxidation.

Chemical aging of organic aerosol (OA) through multiphase oxidation reactions can alter their cloud condensation nuclei (CCN) activity and hygroscopicity. However, the oxidation kinetics and OA reactivity depend strongly on the particle phase state, potentially influencing the hydrophobic-to-hydrophilic conversion rate of carbonaceous aerosol. Here, amorphous Suwannee River fulvic acid (SRFA) aerosol particles, a surrogate humic-like substance (HULIS) that contributes substantially to global OA mass, are oxidized by OH radicals at different temperatures and phase states. When oxidized at low temperature in a glassy solid state, the hygroscopicity of SRFA particles increased by almost a factor of two, whereas oxidation of liquid-like SRFA particles at higher temperatures did not affect CCN activity. Low-temperature oxidation appears to promote the formation of highly-oxygenated particle-bound fragmentation products with lower molar mass and greater CCN activity, underscoring the importance of chemical aging in the free troposphere and its influence on the CCN activity of OA.

1. Introduction

Due to projected increases in organic carbon content in atmospheric aerosols, and corresponding reductions in particulate sulfate, understanding the formation mechanisms and impacts of OA on climate and air quality are becoming increasingly important [*von Schneidemesser et al.*, 2015]. Aerosol particles affect the radiative budget and hydrological cycle directly and through cloud formation [*Stocker et al.*, 2013], and can adversely impact human health [*Kim et al.*, 2015]. Modifications to the physical and chemical properties of OA particles through processes such as multiphase oxidation play a central role in their lifecycle and chemical aging [*Pöschl and Shiraiwa*, 2015]. Especially important are the interactions between OA and reactive trace gases such as O_3, OH, and NO_3, which affect the volatility, oxidation state, size, and hygroscopicity or CCN and ice nuclei activity of aerosol particles [*Farmer et al.*, 2015; *Kroll et al.*, 2015; *Slade et al.*, 2015; *Wang and Knopf*, 2011]. In general, chemical aging through OA oxidation enhances CCN activity due to the formation of more polar and hydrophilic functional groups in the particles, increasing their solubility in water and affecting the surface tension of cloud droplets [*Farmer et al.*, 2015]. However, the effects of chemical aging on CCN concentrations are complex and not easy to quantify in atmospheric models. Global model studies of CCN concentration [*Spracklen et al.*, 2011] and aerosol hygroscopicity [*Pringle et al.*, 2010] have reported low biases compared to observations and large variability, particularly over land and in regions with high OA mass loadings. Some studies achieved closure with measured aerosol hygroscopicity by incorporating the effects of chemical aging [*Asa-Awuku et al.*, 2011; *Crosbie et al.*, 2015] while others found that CCN concentrations are not particularly sensitive to such effects [*Lee et al.*, 2013]. Overall, the available studies suggest potentially important but not yet well understood impacts of OA chemical aging, meriting further investigation. Potentially

important are the roles of temperature and particle phase state modulated by ambient temperature and relative humidity (RH) in governing the degree that particles are oxidized by trace gases [*Shiraiwa et al.*, 2011; *Slade and Knopf*, 2014]. Gases can diffuse faster in liquid particles than in solid particles, impacting reactive uptake and particle oxidation state [*Pöschl and Shiraiwa*, 2015], an important determinant of CCN activity [*Suda et al.*, 2014]. Furthermore, previous studies, see *Kroll et al.* [2015] and references therein, have indicated that OA oxidation reactions shift from a largely functionalization-dominated regime (i.e., addition of C–OH, C=O, and C–OOH functional groups) to fragmentation (i.e., breaking of carbon–carbon bonds) as the particle-phase organics continuously undergo oxidation. While this shift in the chemistry is known to impact the CCN activity of OA [*Harmon et al.*, 2013], fragmentation has been observed to be more prevalent in a solid particle phase state [*Renbaum and Smith*, 2009], and a connection between particle phase, chemistry, and CCN activity has not been made. Considering that accumulation mode OA can reside in the atmosphere for several weeks at varying temperature and RH, and given the often complex but evolving composition of atmospheric aerosol [*Donahue et al.*, 2014] and its CCN activity [*Pringle et al.*, 2010], the CCN activity of OA and resulting cloud droplet numbers could significantly depend on the temperature, RH and thus phase state at which the particles undergo oxidation.

Here we investigate the hygroscopicity of SRFA particles following OH oxidation in an aerosol flow reactor at temperatures ranging from 277 K to 322 K. SRFA has a glass transition temperature (T_g) of about 309 K under dry conditions (RH=0%), which decreases with increasing RH [*Wang et al.*, 2012], and therefore can exhibit various phase states. We present strong evidence that the organic particle phase state, governed by changes in ambient temperature, can

influence the hygroscopicity of OA when oxidized by OH radicals, in turn significantly affecting cloud droplet number concentrations.

2. Methods

The experimental setup and procedures follow our earlier study [*Slade et al.*, 2015]. The setup consists of a horizontally-mounted aerosol flow reactor (AFR) coupled to a cloud condensation nucleus counter (CCNc). In short, pure polydisperse SRFA (IHSS) particles were generated via atomization of 1 wt. % aqueous solution of SRFA in Millipore water (resistivity >18.2 MΩ cm). The particles were subsequently dried prior to entering the flow reactor (relative humidity range of 5% to 15%), which was conditioned with a humidified flow of clean, particle-free air and ultra-high purity N_2/O_2. The relative humidity in the AFR ranged from 32-45% between experiments, and the residence time, t, was maintained ~30 s. The temperature of the flow reactor was controlled by a cooling jacket and was systematically varied from 277 K to 322 K. Under these experimental conditions, the initially dried SRFA particles hydrate in the flow reactor and increase in diameter by ~5% [*Chan and Chan*, 2003]. Given the similarities in the hygroscopic properties of SRFA and levoglucosan (compare, e.g., *Chan and Chan* [2003] and *Chan et al.* [2005]), we expect that the water diffusion timescale is sufficiently rapid (< 100 ms) under the applied flow reactor relative humidity [*Price et al.*, 2014] so that there is no significant hysteresis in particle size or phase along the length of the flow reactor. On average, however, the particle size mode was 60 nm and the size distribution ranged from ~20 nm to 250 nm, and the number concentrations of particles between all of the experiments ranged from $1\text{-}1.4\times10^4$ cm^{-3}.We note that the particle phase was not experimentally evaluated here, instead our interpretation of particle phase as a function of temperature relies on the established *literature* of

the SRFA glass transition temperature T_g, taken as 309 K at 0% RH, but corrected for RH [*Wang et al.*, 2012].

OH radicals were generated via the reaction $O(^1D) + H_2O \rightarrow 2\ OH$, following O_3 photolysis in the AFR using a 60-cm Hg pen-ray ozone-free lamp (Jelight). OH concentrations were calculated applying a photochemical box model and ranged from $0\text{-}2\times10^{10}$ molecule cm^{-3}. The box model and thus OH concentrations were independently verified based on measurements of the loss of isoprene in the presence of OH using a proton transfer reaction time-of-flight mass spectrometer in a separate set of experiments conducted at room temperature [*Slade and Knopf*, 2013]. It is important to note that temperature-dependent reaction rate coefficients were incorporated in the box model and the temperature of the flow reactor was used in the model to evaluate the concentration of OH at each temperature. A detailed analysis of potential additional losses to OH from gas-phase reactions, which is found to be marginal, is provided in the Supporting Information. Uncertainties in the range of OH exposure, however, for each experiment can be a result of drift in the concentration of O_3, residence time, and RH. The most significant uncertainty in the calculated [OH] was associated with a drift in the RH of ±~5%, or roughly a ±10% uncertainty in the calculated [OH], which was largely due to a steady decrease in the diffusion dryer efficiency over the course of an experiment and drift in gas flows due to particle accumulation at the head of a filter (dilution stage) before the particles entered the AFR. Under these conditions, OH exposures, defined as [OH]×t, ranged from $0\text{-}7\times10^{11}$ molecule cm^{-3} s, which corresponds to a maximum 12-hr daytime OH exposure of ~8 d at a background [OH]~2×10^6 molecule cm^{-3}. We note that under these levels of OH exposure, there were neither significant changes to the particle size distribution nor indication of particle volatilization and dependence on temperature, as determined by changes in the total particle volume concentration

with OH exposure level [*Kessler et al.*, 2012; *Slade et al.*, 2015]. In the supplementary material, Fig. S4 shows the average particle size distributions for each exposure experiment, and Fig. S5 shows the total volume concentration for each scan of the particle size distribution. There is some indication that particle volatilization may have occurred based on the decrease in the total volume concentration shown in Fig. S5 when the particles were not oxidized and then immediately oxidized by OH. However, this decrease is not statistically significant compared to the overall variability in volume concentration over the course of experiments, consistent with the observation by *Kessler et al.* [2012] that OH oxidation of SRFA leads to negligible particle volatilization, and therefore is not expected to significantly change the particle size to affect the particle hygroscopicity.

The CCN-derived hygroscopicity of SRFA particles was determined applying κ-Köhler theory [*Petters and Kreidenweis*, 2007]. Briefly, the polydisperse SRFA particle size distributions were scanned at four supersaturations, S=0.2, 0.27, 0.35, and 0.425% to determine the critical particle diameter, i.e., where 50% of the particle population become CCN, defined as $D_{p,50}$. Subsequently, the measured critical diameters at each supersaturation were used to calculate κ as shown in Eqs. 1 and 2.

$$(1)\ \kappa = \frac{4A^3}{27D_{p,50}^3 \ln^2 S},$$

where

$$(2)\ A = \frac{4\sigma M_w}{RT\rho_w}.$$

We assume that upon activation, the CCN are sufficiently dilute, in which case the surface tension σ, molecular weight M_w, and density ρ_w of the particles are derived from water. Prior to

activation, the oxidized particles are assumed to exhibit different composition for different particle sizes, but for the same size, exhibit the same composition. Thus, although the particle population is polydisperse, scanning the population over several supersaturation points enables a direct evaluation of the impact of particle size on the derived κ following exposure to OH [*Slade et al.*, 2015]. The reported κ values are the average of at least four scans of the particle size distribution (two up and two down scans) at each supersaturation. The reported uncertainties in κ are attributed to one standard deviation in the mean of the derived κ.

The kinetic multi-layer model of gas-particle interactions in aerosols and clouds (KM-GAP) [*Shiraiwa et al.*, 2012] has been applied to assess the impact of molecular diffusivity on the condensed phase product concentration profile between OH and SRFA. KM-GAP consists of multiple compartments and layers: gas phase, near-surface gas phase, sorption layer, surface layer, and a number of bulk layers. In the simulation of the aerosol flow tube the aerosol number concentration was 5×10^3 cm^{-3} and the initial particle radius was 100 nm described by 50 bulk layers. KM-GAP treats the following processes of mass transport and chemical reaction explicitly: gas-phase diffusion, surface adsorption and desorption, surface–bulk exchange, bulk diffusion, and chemical reactions in the gas phase, at the surface and in the particle bulk. The required kinetic parameters, such as condensed-phase reaction rate coefficients, surface accommodation coefficient and desorption lifetime, were adopted from the system of OH uptake by levoglucosan [*Arangio et al.*, 2015] assuming that SRFA and levoglucosan have similar reactivity, as indicated by their nearly equivalent reactive uptake coefficients [*Kessler et al.*, 2012] and listed in Table S1. The temporal evolution of the gas-phase, surface and bulk compositions were simulated by numerically solving the ordinary differential equations considering the mass balance of each layer. Here, two reaction products were considered, one

being volatile (glucic acid) and the other one nonvolatile (1,3-dioxolane-2,4-dione) as suggested by the reaction mechanism proposed in *Slade and Knopf* [2013] for OH uptake by levoglucosan. The second-order gas-phase reaction rate coefficient between OH and volatile products was assumed to be in the range of 10^{-13} – 10^{-10} cm^3 s^{-1} to take into account a further hydrogen abstraction step by OH radical from glucic acid in the gas-phase. KM-GAP predicted very little size change in the reaction time of ~30 s, which is consistent with size distribution and volume concentration measurements (Figs. S4 and S5).

The cloud parcel model used in this study contains a detailed spectral description of cloud microphysics and has implemented the κ-Köhler approach to describe the CCN activation (for details see *Reutter et al.* [2009] and references therein. The model simulations were performed using parameters characteristic for biomass burning aerosol [*Andreae et al.*, 2004; *Janhall et al.*, 2010]: particle number concentration of 1000-10000 cm^{-3}; the number size distribution has one log-normal mode with geometric mean diameter of 150 nm and a standard deviation of 1.4.

3. Results and Discussion

We first evaluate the CCN activity or hygroscopicity, κ, of pure SRFA particles in the absence of OH. The derived κ values and measured critical particle diameters for pure SRFA particles acquired under different supersaturations are shown in Supporting Information (SI) Table S2. The derived κ of pure SRFA particles at all investigated supersaturations ranges from 0.041 to 0.055, which is within the uncertainty of previous measurements [*Chan and Chan*, 2003].

Evidence for significant enhancement in the CCN activity of SRFA particles following OH exposure was observed for all of the applied supersaturations, as shown in Fig. 1, which depicts κ (top row) and $D_{p,50}$ (bottom row) as a function of OH exposure and temperature (color scale)

for each supersaturation. At maximum, for particles 120 nm or less in diameter, κ nearly doubles following exposure to OH, particularly at temperatures below ~295 K, whereas there is no increase in κ at temperatures >300 K. Due to differences in the surface-to-volume ratios between larger particles (activated at lower supersaturation) and smaller particles (activated at higher supersaturation), the particle oxidation level and thus increase in κ as a function of OH exposure can depend on the particle size [*Slade et al.*, 2015]. This surface-to-volume effect on the derived κ following OH oxidation is represented in Fig. S6; for the same experimental conditions, as the activated particle size decreases with increasing supersaturation, the smaller particles exhibit relatively larger κ. However, the variation in κ for the same supersaturation and experimental conditions is not as significant as the change in κ resulting from a change in temperature under the same conditions. This suggests for any supersaturation, κ is more impacted by changes in temperature at the same OH exposure than by the variability in particle size.

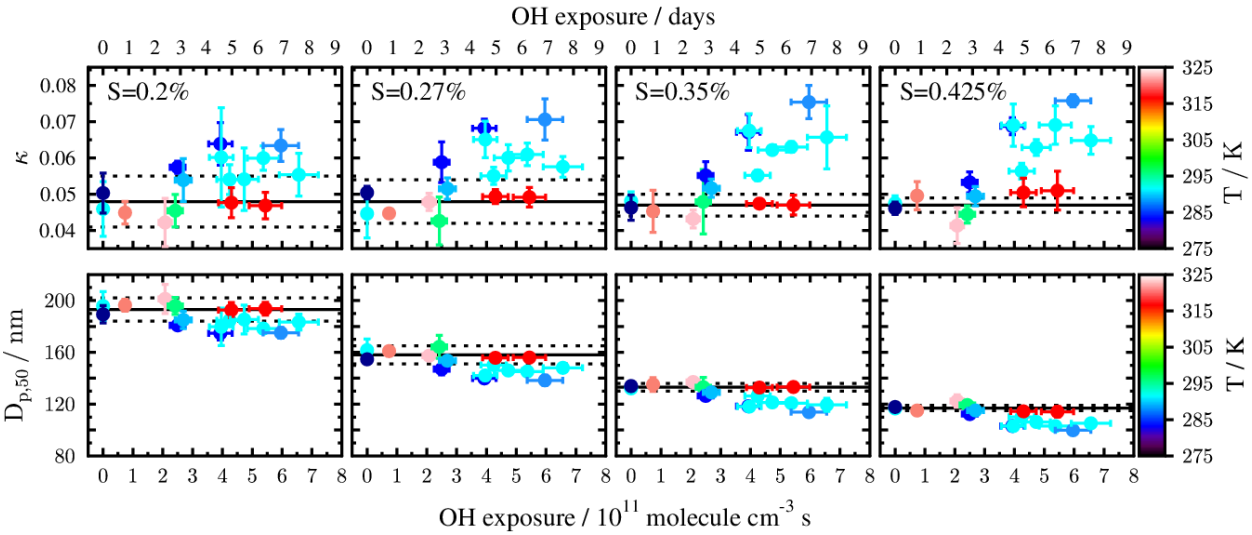

Figure 1. SRFA hygroscopicity (top panels) and activation diameters (bottom panels) as a function of OH exposure and temperature (color scale) at different supersaturations as given in legends. The reported data points are the averaged derived κ and $D_{p,50}$, and the uncertainty

represents one standard deviation from the mean. The horizontal error bars correspond to a 10% uncertainty in the calculated OH concentrations. The solid and dashed black lines represent the averaged derived κ or $D_{p,50}$ and one standard deviation from the mean in the absence of OH, respectively, derived from Table S1.

Since previous studies of OA oxidation and their effects on CCN activity were conducted at fixed (near room) temperature, we do not have the means for a direct mechanistic comparison. However, based on the applied temperature range and RH of 32-45%, SRFA particles are glassy or highly-viscous semisolids below ~295 K, and liquid-like above ~300 K [*Wang et al.*, 2012]. According to recent studies, a change in particle phase state can affect the degree of oxidant uptake by similar amorphous OA particles, suggesting greater uptake for lower particle viscosity (above T_g) and less uptake for higher particle viscosity (below T_g). However, it appears that the rate of OH uptake does not have a significant impact on particle hygroscopicity since above T_g, there was no change in κ with increasing OH exposure. More importantly, it appears that at temperatures below T_g, there is a greater propensity to achieve multiple generations of oxidation of the same molecule, resulting in fragmentation. A sensitivity analysis applying KM-GAP [*Shiraiwa et al.*, 2012] reveals that the first-generation oxidation products of SRFA are largely confined to the particle surface below T_g when the particles are glassy, whereas in liquid particles (above T_g) the reaction products can rapidly diffuse into the bulk, as shown in Fig. S3. On glassy particles, the first-generation products are thus concentrated at the surface where they remain fully exposed to oxidants and undergo rapid further oxidation and fragmentation, yielding highly-oxygenated products with lower molar mass. In contrast, the first generation products in liquid particles are quickly transported into the bulk, and are less likely to undergo further oxidation and fragmentation. The oxidation of SRFA and similar compounds comprised of

oxidized, branched and cyclical structures, generally results in stronger chemical fragmentation [*Kroll et al.*, 2015], and recent work indicates the OH oxidation of laboratory-generated SRFA aerosol leads to fragmentation and an enhancement in its carbon oxidation state [*Kessler et al.*, 2012]. Furthermore, more multiply-oxidized species as well as low-molecular-weight species have been detected from the radical-initiated oxidation of solid rather than liquid particles of the same composition [*Renbaum and Smith*, 2009]. Assuming the chemistry is similar for SRFA, it is possible that there is a greater abundance of multiply-oxidized fragmentation products when SRFA is oxidized below T_g.

Highly-oxygenated and fragmented compounds can impact the physicochemical properties of OA particles by increasing the carbon oxidation state [*Kessler et al.*, 2012], lowering the average particle molar mass, increasing the solubility, and reducing the surface tension [*George et al.*, 2009]. Since saturation vapor pressure is a strong function of temperature, oxidation products with lower mass are also less likely to evaporate at lower temperature [*Topping et al.*, 2013]. As summarized in Fig. 2, experimentally-derived κ is plotted as a function of flow reactor temperature and equivalent atmospheric OH exposure assuming a 12-hr daylight exposure of [OH]=2×10^6 molecules cm^{-3}.

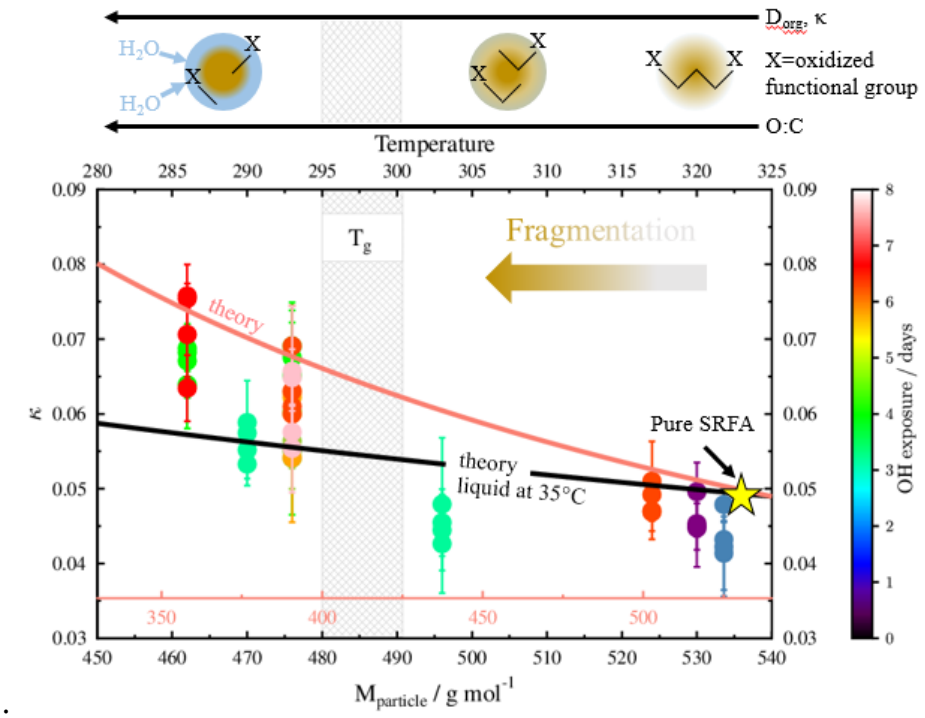

Figure 2. Hygroscopicity parameter, κ, as a function of temperature upon oxidation of Suwannee River fulvic acid (SRFA) particles by OH radicals. Color coding represents the equivalent tropospheric OH exposure in days. The black curve shows κ derived from Eq. (3) and corresponds to the average particle molar mass expected following OH oxidation of SRFA (bottom x-axis), as discussed in the Supporting Information. The pink curve represents theoretical κ and corresponds to the range in molar mass on the pink inset axis. The star indicates on the curve where κ corresponds to the approximate molar mass of SRFA (535 g mol^{-1}) based on the derived κ of pure SRFA and Eq. (3). The gray shaded region shows the glass transition range of SRFA accounting for the effects of slight changes in RH among different experiments. Uncertainty bars represent 1σ from the mean in the derived κ. The conceptual illustration at the top, from right-to-left, shows a particle undergoing a glassy phase transition at constant OH exposure. The condensed phase organics (indicated by the skeletal structure, where X represents any oxidized functional group, i.e., -OH, =O, -OOH, etc.) undergo greater fragmentation with

increasing viscosity in the presence of OH, increasing O:C. Below T_g, the oxygenated fragmentation products that remain in the condensed phase enhance the hygroscopicity of the particle, indicated by more liquid water (blue) in the particle.

It is clear that only when SRFA is oxidized at temperatures below its glass transition (indicated by the gray region in Fig. 2), experimentally-derived κ increases by almost a factor of two at the highest OH exposure, whereas no significant enhancement relative to pure SRFA occurs above T_g. There are likely two major mechanisms at play impacting the observed changes to κ that we will explore further here: (1) that involving a reduction in the average particle molar mass due to the presence of highly-oxygenated fragmentation products and (2) surface tension suppression.

Analyses based on κ-Köhler theory indicate that κ can be approximated as a function of both the density and molar mass of the solute as follows [*Mikhailov et al.*, 2013]:

$$(3)\ \kappa_i = J_i \frac{\frac{\rho_i}{M_i}}{\frac{\rho_w}{M_w}},$$

where J_i is the van't Hoff factor and ρ and M refer to the density and molar mass of the solute (i) and water (w), respectively. Therefore, the effects on κ due to a reduction in molar mass at constant particle density as a result of fragmentation can be evaluated using Eq. (3). Applying the measured κ of pure SRFA, J_i=1 and ρ=1.47 g cm^{-3} [*Wang et al.*, 2012], we derive a pure SRFA molar mass of 535 g mol^{-1}, within the range of previous estimates [*Dinar et al.*, 2006]. Previous work has shown that the carbon oxidation state of SRFA increases with fragmentation following exposure to OH when the particles are oxidized in a liquid-like state at 35°C [*Kessler et al.*, 2012]. As discussed in the Supporting Information, we estimate that under these conditions, fragmentation reduces the average molar mass of SRFA particles by ~85 g mol^{-1}. As indicated by the black curve in Fig. 2, such a decrease in molar mass can partially explain the

observed increase in κ, but significantly underestimates κ below T_g. To achieve the observed maximum κ of 0.08 requires a reduction in molar mass of ~205 g mol^{-1}, as indicated by the pink curve. Whether fragmentation reduces the particle molar mass to such a degree in a glassy solid state is unclear since it was not determined experimentally. However, we expect greater fragmentation, and thus lower molar mass, in the solid glassy particles, similar to the observation by *Renbaum and Smith* [2009] that brassidic acid particles, when oxidized in a solid state, generate smaller and more oxygenated products compared to oxidation in a liquid state.

The effects of surface tension suppression also cannot be neglected. Recent work indicates that the surface tension of atmospheric aerosols can be greatly suppressed due to the presence of concentrated surface-active species [*Ruehl et al.*, 2016]. Heterogeneous OH oxidation was also shown to greatly suppress the surface tension of bis-ethyl-sebacate particles [*George et al.*, 2009]. It is noteworthy that at lower temperatures, the more viscous particles may be conducive for the formation and longevity of surface-active organics, however, requiring further study. Other temperature effects, e.g., wall loss and additional gas-phase reactions, which could influence the OH concentration gradient in the flow reactor and subsequently the OH exposure level are found to have only marginal impacts as discussed in the Supporting Information.

4. Atmospheric Implications

These findings have significant implications for cloud formation and our understanding of OA evolution in the atmosphere. Our results show that multiphase oxidation of HULIS enhances the CCN activity of the aerosol at temperatures below and not above T_g, implying temperature and particle phase state may influence the rate of hydrophobic-to-hydrophilic conversion of OA due to heterogeneous oxidation. While OA species can exhibit very low κ (≤0.01), our results suggest low-temperature OA oxidation can lead to or significantly contribute to the measurement-derived

ambient κ of the organic fraction of ~0.1 [*Gunthe et al.*, 2009; *Pringle et al.*, 2010]. Furthermore, our results indicate that κ may be better constrained when incorporating the observed effects of temperature in atmospheric models that show discrepancies with measured κ in regions with high OA mass loadings [*Pringle et al.*, 2010].

It is also important to note that the impact of clouds on Earth's energy balance partially depends on the number and size of droplets and ice crystals they contain. Here we apply a cloud parcel model to test the sensitivity of cloud droplet number concentrations (CDNC) on increasing κ by low-temperature oxidation. We calculate that an increase in OA particle hygroscopicity as observed upon oxidation of SRFA in a glassy solid state can account for up to 5% to 27% greater cloud droplet number concentrations (CDNC) compared to oxidation of SRFA in a liquid-like state, depending on the updraft velocity and initial aerosol number concentration, as depicted in Fig. 3.

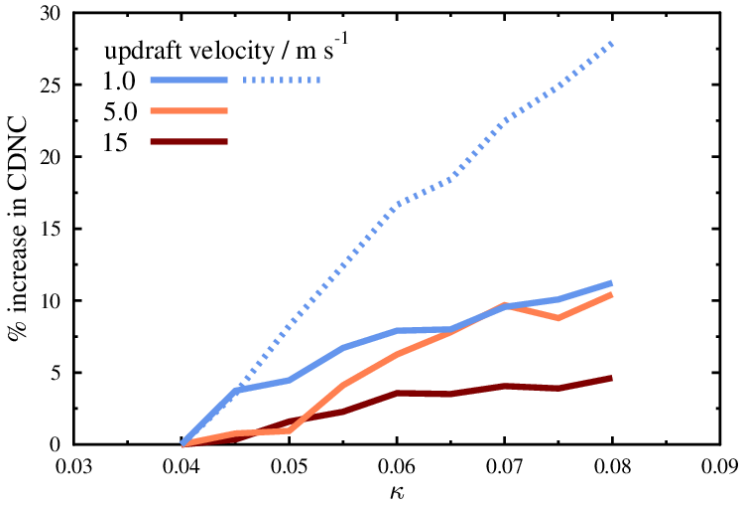

Figure 3. Change in cloud droplet number concentration (CDNC) as a function of hygroscopicity, κ, and updraft velocity. The model assumes an initial aerosol number concentration for that typical of biomass burning plumes of 10^4 cm^{-3}, particle density of 1.4 g

cm^{-3}, and particle diameter of 150 nm, except the dashed line, which assumes an initial number concentration of 10^3 cm^{-3}.

The calculated potential increase of CDNC due to chemical aging and increasing hygroscopicity of OA may have important implications for the hydrological cycle and climate because cloud droplet numbers affect the microphysical and optical properties of clouds. Such effects may be particularly relevant for regions and periods where CCN concentrations are dominated by OA particles, such as tropical forest regions during pristine conditions in the wet season [*Hodzic et al.*, 2016]. Globally, the chemical aging effects in our study could be important for understanding the uncertainties in radiative climate forcing associated with natural aerosols during the pre-industrial era [*Carslaw et al.*, 2013] when there were greater proportions of OA and less particulate sulfate and nitrate [*Tsigaridis et al.*, 2006].

5. Conclusions

This study demonstrates that during the oxidative aging process of OA, particle phase state and temperature are important variables to consider for predicting its cloud formation potential. Significant increases in particle hygroscopicity have been observed when oxidation occurred just a few degrees Kelvin below the particle's glass transition temperature. This has been attributed to a reduction in the average particle molar mass due to the presence of highly-oxygenated fragmentation products at the highly viscous particle surface. Concurrently, reductions in surface tension due to the presence of surface-active organics can potentially accelerate the enhancement in hygroscopicity at temperatures below the glass transition of OA. Considering these effects, cloud droplet number concentrations can increase significantly, in turn potentially influencing the hydrological cycle and climate.

It is essential to keep in mind that the mean tropospheric temperature is about 255 K, well below the temperatures of most laboratory experiments and the T_g of many other relevant amorphous OA species [*Koop et al.*, 2011]. Considering the phase state of particles can influence the formation, growth, and partitioning of secondary organic aerosol (SOA), water uptake, ice nucleation, and the long-range transport of toxic organic substances [*Pöschl and Shiraiwa*, 2015], further investigations are needed to fully understand the impact that temperature-modulated particle phase has on the chemical composition, CCN activity, and climate effects of atmospheric OA.

References

Andreae, M. O., D. Rosenfeld, P. Artaxo, A. A. Costa, G. P. Frank, K. M. Longo, and M. A. F. Silva-Dias (2004), Smoking rain clouds over the Amazon, *Science*, *303*(5662), 1337-1342.

Arangio, A. M., J. H. Slade, T. Berkemeier, U. Poschl, D. A. Knopf, and M. Shiraiwa (2015), Multiphase chemical kinetics of OH radical uptake by molecular organic markers of biomass burning aerosols: humidity and temperature dependence, surface reaction, and bulk diffusion, *J. Phys. Chem. A*.

Asa-Awuku, A., et al. (2011), Airborne cloud condensation nuclei measurements during the 2006 Texas Air Quality Study, *J. Geophys. Res.-Atmos.*, *116*.

Carslaw, K. S., et al. (2013), Large contribution of natural aerosols to uncertainty in indirect forcing, *Nature*, *503*(7474), 67-71.

Chan, M. N., and C. K. Chan (2003), Hygroscopic properties of two model humic-like substances and their mixtures with inorganics of atmospheric importance, *Environ. Sci. Technol.*, *37*(22), 5109-5115.

Chan, M. N., M. Y. Choi, N. L. Ng, and C. K. Chan (2005), Hygroscopicity of water-soluble organic compounds in atmospheric aerosols: Amino acids and biomass burning derived organic species, *Environ Sci Technol*, *39*(6), 1555-1562.

Crosbie, E., J. S. Youn, B. Balch, A. Wonaschutz, T. Shingler, Z. Wang, W. C. Conant, E. A. Betterton, and A. Sorooshian (2015), On the competition among aerosol number, size and composition in predicting CCN variability: a multi-annual field study in an urbanized desert, *Atmos. Chem. Phys.*, *15*(12), 6943-6958.

Dinar, E., T. F. Mentel, and Y. Rudich (2006), The density of humic acids and humic like substances (HULIS) from fresh and aged wood burning and pollution aerosol particles, *Atmos. Chem. Phys.*, *6*, 5213-5224.

Donahue, N. M., A. L. Robinson, E. R. Trump, I. Riipinen, and J. H. Kroll (2014), Volatility and aging of atmospheric organic aerosol, *Top. Curr. Chem.*, *339*, 97-143.

Farmer, D. K., C. D. Cappa, and S. M. Kreidenweis (2015), Atmospheric processes and their controlling influence on cloud condensation nuclei activity, *Chem. Rev.*, *115*(10), 4199-4217.

George, I. J., R. Y. W. Chang, V. Danov, A. Vlasenko, and J. P. D. Abbatt (2009), Modification of cloud condensation nucleus activity of organic aerosols by hydroxyl radical heterogeneous oxidation, *Atmos. Environ.*, *43*(32), 5038-5045.

Gunthe, S. S., et al. (2009), Cloud condensation nuclei in pristine tropical rainforest air of Amazonia: size-resolved measurements and modeling of atmospheric aerosol composition and CCN activity, *Atmos. Chem. Phys.*, *9*(19), 7551-7575.

Harmon, C. W., C. R. Ruehl, C. D. Cappa, and K. R. Wilson (2013), A statistical description of the evolution of cloud condensation nuclei activity during the heterogeneous oxidation of squalane and bis(2-ethylhexyl) sebacate aerosol by hydroxyl radicals, *Phys. Chem. Chem. Phys.*, *15*(24), 9679-9693.

Hodzic, A., P. S. Kasibhatla, D. S. Jo, C. D. Cappa, J. L. Jimenez, S. Madronich, and R. J. Park (2016), Rethinking the global secondary organic aerosol (SOA) budget: stronger production, faster removal, shorter lifetime, *Atmos. Chem. Phys.*, *16*, 7917-7941.

Janhall, S., M. O. Andreae, and U. Pöschl (2010), Biomass burning aerosol emissions from vegetation fires: particle number and mass emission factors and size distributions, *Atmos. Chem. Phys.*, *10*(3), 1427-1439.

Kessler, S. H., T. Nah, K. E. Daumit, J. D. Smith, S. R. Leone, C. E. Kolb, D. R. Worsnop, K. R. Wilson, and J. H. Kroll (2012), OH-initiated heterogeneous aging of highly oxidized organic aerosol, *J. Phys. Chem. A*, *116*(24), 6358-6365.

Kim, K.-H., E. Kabir, and S. Kabir (2015), A review on the human health impact of airborne particulate matter, *Environ. Int.*, *74*, 136-143.

Koop, T., J. Bookhold, M. Shiraiwa, and U. Pöschl (2011), Glass transition and phase state of organic compounds: dependency on molecular properties and implications for secondary organic aerosols in the atmosphere, *Phys. Chem. Chem. Phys.*, *13*(43), 19238-19255.

Kroll, J. H., C. Y. Lim, S. H. Kessler, and K. R. Wilson (2015), Heterogeneous oxidation of atmospheric organic aerosol: kinetics of changes to the amount and oxidation state of particle-phase organic carbon, *J. Phys. Chem. A*, *119*(44), 10767-10783.

Lee, L. A., K. J. Pringle, C. L. Reddington, G. W. Mann, P. Stier, D. V. Spracklen, J. R. Pierce, and K. S. Carslaw (2013), The magnitude and causes of uncertainty in global model simulations of cloud condensation nuclei, *Atmos. Chem. Phys.*, *13*, 8879-8914.

Mikhailov, E., S. Vlasenko, D. Rose, and U. Pöschl (2013), Mass-based hygroscopicity parameter interaction model and measurement of atmospheric aerosol water uptake, *Atmos. Chem. Phys.*, *13*(2), 717-740.

Petters, M. D., and S. M. Kreidenweis (2007), A single parameter representation of hygroscopic growth and cloud condensation nucleus activity, *Atmos. Chem. Phys.*, *7*(8), 1961-1971.

Pöschl, U., and M. Shiraiwa (2015), Multiphase chemistry at the atmosphere-biosphere interface influencing climate and public health in the anthropocene, *Chem. Rev.*, *115*, 4440-4475.

Price, H. C., B. J. Murray, J. Mattsson, D. O'Sullivan, T. W. Wilson, K. J. Baustian, and L. G. Benning (2014), Quantifying water diffusion in high-viscosity and glassy aqueous solutions using a Raman isotope tracer method, *Atmos. Chem. Phys.*, *14*, 3817–3830.

Pringle, K. J., H. Tost, A. Pozzer, U. Pöschl, and J. Lelieveld (2010), Global distribution of the effective aerosol hygroscopicity parameter for CCN activation, *Atmos. Chem. Phys.*, *10*, 5241-5255.

Renbaum, L. H., and G. D. Smith (2009), The importance of phase in the radical-initiated oxidation of model organic aerosols: reactions of solid and liquid brassidic acid particles, *Phys. Chem. Chem. Phys.*, *11*(14), 2441-2451.

Reutter, P., H. Su, J. Trentmann, M. Simmel, D. Rose, S. S. Gunthe, H. Wernli, M. O. Andreae, and U. Poschl (2009), Aerosol- and updraft-limited regimes of cloud droplet formation: influence of particle number, size and hygroscopicity on the activation of cloud condensation nuclei (CCN), *Atmos. Chem. Phys.*, *9*(18), 7067-7080.

Ruehl, C. R., J. F. Davies, and K. R. Wilson (2016), An interfacial mechanism for cloud droplet formation on organic aerosols, *Science*, *351*, 1447-1450.

Shiraiwa, M., M. Ammann, T. Koop, and U. Pöschl (2011), Gas uptake and chemical aging of semisolid organic aerosol particles, *P. Natl. Acad. Sci. USA*, *108*(27), 11003-11008.

Shiraiwa, M., C. Pfrang, T. Koop, and U. Pöschl (2012), Kinetic multi-layer model of gas-particle interactions in aerosols and clouds (KM-GAP): linking condensation, evaporation and chemical reactions of organics, oxidants and water, *Atmos. Chem. Phys.*, *12*(5), 2777-2794.

Slade, J. H., and D. A. Knopf (2013), Heterogeneous OH oxidation of biomass burning organic aerosol surrogate compounds: assessment of volatilisation products and the role of OH concentration on the reactive uptake kinetics, *Phys. Chem. Chem. Phys.*, *15*(16), 5898-5915.

Slade, J. H., and D. A. Knopf (2014), Multiphase OH oxidation kinetics of organic aerosol: The role of particle phase state and relative humidity, *Geophys. Res. Lett.*, *41*(14), 5297-5306.

Slade, J. H., R. Thalman, J. Wang, and D. A. Knopf (2015), Chemical aging of single and multicomponent biomass burning aerosol surrogate particles by OH: implications for cloud condensation nucleus activity, *Atmos. Chem. Phys.*, *15*(17), 10183-10201.

Spracklen, D. V., K. S. Carslaw, U. Pöschl, A. Rap, and P. M. Forster (2011), Global cloud condensation nuclei influenced by carbonaceous combustion aerosol, *Atmos. Chem. Phys.*, *11*, 9067-9087.

Stocker, T. F., D. Qin, G. K. Plattner, M. Tignor, S. K. Allen, J. Boschung, A. Nauels, Y. Xia, V. Bex, and P. M. Midgley (2013), *Climate Change 2013: the Physical Science Basis, contribution of Working Group 1 to the Fifth Assessment Report of the Intergovernmental Panel on Climate Change*, Cambridge University Press, Cambridge, UK and New York, NY, USA.

Suda, S. R., et al. (2014), Influence of functional groups on organic aerosol cloud condensation nucleus activity, *Environ. Sci. Technol.*, *48*(17), 10182-10190.

Topping, D., P. Connolly, and G. McFiggans (2013), Cloud droplet number enhanced by co-condensation of organic vapours, *Nat. Geosci.*, *6*(6), 443-446.

Tsigaridis, K., M. Krol, F. J. Dentener, Y. Balkanski, J. Lathiere, S. Metzger, D. A. Hauglustaine, and M. Kanakidou (2006), Change in global aerosol composition since preindustrial times, *Atmos. Chem. Phys.*, *6*, 5143-5162.

von Schneidemesser, E., et al. (2015), Chemistry and the linkages between air quality and climate change, *Chem. Rev.*, *115*(10), 3856-3897.

Wang, B. B., and D. A. Knopf (2011), Heterogeneous ice nucleation on particles composed of humic-like substances impacted by O_3, *J. Geophys. Res.-Atmos., 116*.

Wang, B. B., A. T. Lambe, P. Massoli, T. B. Onasch, P. Davidovits, D. R. Worsnop, and D. A. Knopf (2012), The deposition ice nucleation and immersion freezing potential of amorphous secondary organic aerosol: Pathways for ice and mixed-phase cloud formation, *J. Geophys. Res.-Atmos., 117*.

Acknowledgements

J. H. Slade and D. A. Knopf acknowledge support from the National Science Foundation grants AGS-0846255 and AGS-1446286. J. Wang acknowledges support from the US Department of Energy's Atmospheric System Research Program (Office of Science, OBER) under contract DE-AC02098CH10886. M. Shiraiwa and A. Arangio acknowledge support from the Max Planck Society. H. Su acknowledges support from the EU project BACCHUS (project number 603445). The experimental data presented in this study can be accessed in the Supplementary Information Tables S1-S3.